Research Article GU J Sci 36(1): 190-206 (2023) DOI: 10.35378/gujs.826149

Gazi University

Journal of Science

http://dergipark.gov.tr/gujs

A Sliding-Mode Control with Efficient Chattering Alleviation for Single-Phase Voltage Source Inverters

Farzaneh BAGHERI[1], Hasan KOMURCUGIL[2]

[1]*Antalya Bilim University, Department of Electrical and Electronics Engineering, Antalya, Turkey*
[2]*Eastern Mediterranean University, Department of Computer Engineering, Famagusta, via Mersin 10, Turkey*

Highlights

- This paper focuses on an efficient scheme to alleviate the chattering of the sliding mode control.
- A variable boundary layer is proposed for tackling the chattering.
- A comparison of different schemes is presented to show the outperformance of the proposed method.

Article Info

Received: 15 Nov 2020
Accepted: 18 Feb 2022

Keywords

Chattering suppression
Variable boundary Layer
Sliding mode control
Voltage source inverter

Abstract

This paper presents an adaptive sliding mode control (SMC) method with a variable boundary layer for single-phase voltage source inverters. This strategy offers a very simple sliding function without any derivative term while preserving unique characteristics of the sliding mode control like fast dynamic response and robustness against parameter variations while also possessing the variable boundary layer method to reject the chattering phenomena. Chattering excites the high frequencies in the system and leads to inaccuracy and instability. It is shown that despite the conventinal approches, the proposed variable boundary layer method can both alleviate the chattering and generating the minimum steady state error. Owing to the adaptive nature of the suggested control approach which adjusts the thickness of the boundary layer, the whole mechanism can be controlled successfully under unpredictable parameter variations. The accomplishment of the suggested strategy is investigated by simulations in MATLAB/Simulink. The outcomes are compared with the outcomes obtained without boundary layer, with constant boundary layer and super twisting sliding control methods. The comparison reveals that the proposed control technique outperforms the other control methods for the voltage source inverter. The results demonstrate that while the conventional, SMC with constant boundary layer and super twisting sliding control (STSMC) methods have 50% ,8% and 10% chattering over their control input respectively, the proposed method has less than 3% chattering over the control input.

1. INTRODUCTION

Recently, the widespread development of the renewable energy sources namely wind, solar panels, and fuels cells have led to a marvelous surge in the use of voltage source inverters (VSIs) [1-3]. Although the grid connected voltage source inverters are very popular, the standalone voltage source inverters like uninterruptable power supplies (UPS) and voltage regulation systems are also widely used in the industry. UPS should supply critical and nonlinear loads while preserving sinusoidal output voltage tracking the referenced frequency and amplitude with low total harmonic distortion (THD) in steady state and transients. Thus, the control methodology developed for such a system should have fast dynamic response against abrupt changes in the load, robustness against all disturbances and low (or preferably zero) steady state error.

Overview of literature shows that various methods have focused on the control of voltage source inverters. These methods can be divided into two groups: nonlinear control methods and linear control methods. The linear control methods are proportional–integral-derivative (PID) control and proportional–resonant (PR)

*Corresponding author, e-mail: farzaneh.bagheri@antalya.edu.tr

control [4-5] strategies and the nonlinear methods are repetitive control (RC) [6-8], hysteresis current control [9], H_∞ control [10], deadbeat control [11-13], feedback control [14-15], internal model control [16], and sliding mode control schemes [17-26].

Due to intrinsic characteristics of the power electronics-based converters, the linear control methods are not sufficiently capable to manage the behavior of the inverter under dynamic disturbances however they perform satisfactorily in steady state.

Among the nonlinear strategies, the RC method is not robust enough against uncertainties because it needs exact knowledge of the system parameters. Although the hysteresis current control method can be easily implemented in practice, it suffers from the limitless switching frequency. On the other hand, the major disadvantages of the H_∞ control technique are the implementation complexity due to the extensive mathematical equations and requirement of system's average model. Deadbeat control is not desirable method due to its high sensitivity to the parameter variations which leads to oscillatory response. On the other hand, even though the mentioned control methods yield acceptable response in the stable time periods for nonlinear loads, but the results during the transient changes are not satisfactory.

Due to the aforementioned problems, the nonlinear control methods for instance the sliding mode control (SMC) are widely used to control the converters in power electronics. Due to the intrinsic switching essence of the power electronic converters, the SMC is well-matched to the inverters. However, the SMC suffers from chattering phenomenon which is undesirable due to high control activity and exciting high frequency because of the dynamics neglected in the system modeling.

Numerous schemes are proposed to eliminate or lessen the destructive effects of the chattering [17-24]. The chattering alleviation methods proposed in [17] are designed to achieve a quasi-sliding mode instead of an ideal sliding mode which can lead to steady state error and can be leveraged for all electromechanical systems. Since the power converters need to work with a bounded switching frequency, most of the methods proposed in [17] can be applied on the power converters to compensate the high oscillations. Among the proposed methods, the boundary layer strategy is more practical than the others for the power converters to alleviate chattering and smooth the control input because of its simplicity in theory and implementation.

In [18], the boundary layer SMC is applied to the single-phase voltage source inverter which is based upon smoothing the sliding manifold inside a constant boundary layer with a fixed boundary layer thickness. However, it achieves robustness in finite time, but leads to a large steady state error in the load voltage. To tackle the large steady state error because of a fixed boundary layer thickness, the variable boundary layer method is proposed in [19]. In this paper, a variable boundary layer SMC is proposed for compliant joint manipulators in industrial robots which is based on defining a variable first order boundary layer method with an expanding factor. Nevertheless, the expanding factor is a constant value which is not adaptive to the disturbances of the system and should be manually regulated under transient situations.

The high order sliding mode control (HOSMC) is also another method, first suggested in [20] to alleviate the chattering oscillations and soon after that high rate of publications in the application of HOSMC in power electronics emerged in literature [21-24]. In [21], a super twisting sliding mode control (STSMC) is introduced for single-phase photovoltaic grid-connected voltage source inverters. The control input is considered as the summation of an equivalent control input and the super twisting control. The results of the state space variables and the sliding functions show that the chattering is removed significantly however there is a confliction between the control input waveform and the sliding function waveform in chattering alleviation.

A sliding mode control scheme based on a super-twisting control input for the three-phase AC/DC converter is proposed in [22] to improve the dynamic response of the system under disturbances instead of using the conventional PI controllers and the chattering elimination is not discussed in detail. In [23], a super twisting algorithm is proposed for a droop-controlled inverter to use the merits of this method in disturbance rejections. However, the results show that the transient behavior, the disturbance elimination, and tracking

the reference are enhanced but the research has not studied the chattering suppression. On the other hand, the authors have used the boundary layer method with the super twisting algorithm to tackle the chattering phenomena.

Vadim Utkin has also released a discussion on the capability of the HOSMC method to remove the chattering and has compared the STSMC to the conventional sliding mode control method [25]. He concluded that the chattering in HOSM control is more than conventional method. However, he reported that this method can show different behavior in different systems. Furthermore, the HOSM control method is more complex than the conventional ones due to the calculations needed to find the high order derivatives of the sliding manifolds.

Motivated from the variable boundary layer method presented in [19], we have investigated the possibility of applying a variable boundary layer scheme for controlling a single-phase UPS inverter. On the contrary to the other variable boundary layer methods, the boundary layer in the proposed scheme is adaptive to the variations of sliding manifold while also preserving robustness. As a consequence of variable boundary layer, minimum steady state error, quick dynamic response and strong robustness under parameter variations and fixed switching frequency can be obtained. On the other hand, to the best of the authors knowledge, the simplification of the sliding function with the variable boundary layer for bounding the switching frequency has not been utilized for the power electronic systems and specially the voltage source inverts before. In the simulation section, the suggested scheme is compared to the STSMC method, and the results of both methods are discussed consequently.

This paper is organized as follows: in section 2, a mathematical description of the system is demonstrated. In section 3, the sliding mode control method is comprehensively explained. In section 4 the variable boundary layer method for chattering alleviation of the conventional sliding mode control is introduced and mathematically clarified. The reference generation and leveraging a PR controller to generate the inductance current reference is inspected in section 5. The feasibility of the proposed scheme is discussed through simulations in section 6. This section is included of the comparison between different SMC methods and shows the superiority of the proposed scheme over the existing ones. The paper is concluding with a brief conclusion and the advantages of the proposed method in the final section.

2. MATHEMATICAL DESCRIPTION OF THE SYSTEM

A load connected voltage source inverter is shown in Figure 1. The inverter is integrated to the load via a LC filter. The mathematical equations of the system are derived as

$$L\frac{di_L}{dt} = uV_{in} - v_o \tag{1}$$

$$i_C = C\frac{dv_o}{dt} \tag{2}$$

$$i_L = i_C + i_o \tag{3}$$

where u and V_{in} denote the control input and the dc input voltage respectively. Let us consider two state variables in the system as

$$x_1 = i_L - i_L^* \tag{4}$$

$$x_2 = v_o - v_o^*. \tag{5}$$

Then, the state space model of the system can be written as the following, where i_L^* and v_o^* are the filter inductor current and capacitor voltage references

$$\begin{bmatrix} \dot{x}_1 \\ \dot{x}_2 \end{bmatrix} = \begin{bmatrix} 0 & -1/L \\ 1/C & 0 \end{bmatrix} \begin{bmatrix} x_1 \\ x_2 \end{bmatrix} + \begin{bmatrix} V_{in}/L \\ 0 \end{bmatrix} u + W(t) \tag{6}$$

where $W(t)$ is the disturbance term given as

$$W(t) = \begin{bmatrix} \dfrac{-v_o^*}{L} - i_L^* \\ \dfrac{i_L^* - i_o}{C} - \dot{v}_o^* \end{bmatrix}. \tag{7}$$

The first row of the state space model in (6) can be expressed in the form of a general first order equation as follows

$$\dot{x}_1 = f(x_2) + gu + d(t) \tag{8}$$

while the functions can be demonstrated as

$$f(x_2) = -x_2 / L \tag{9}$$

$$g = V_{in} / L \tag{10}$$

$$d(t) = \frac{-v_o^*}{L} - i_L^*. \tag{11}$$

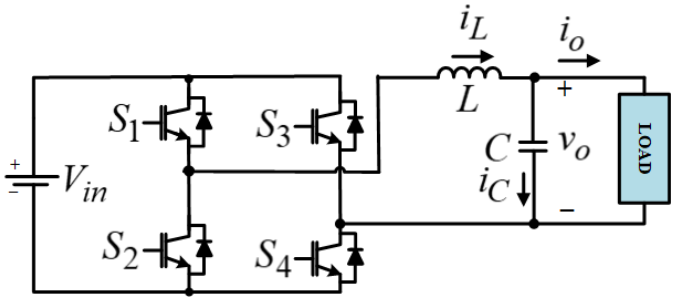

Figure 1. *Single-phase standalone voltage source inverter*

3. SLIDING MODE CONTROL

The ultimate target of applying the sliding control strategy to the load connected inverter is to compel the actual load voltage to follow the load voltage reference under the worst-case circumstances which occur under the turbulences and nonlinear loads. In conventional SMC method, the sliding manifold is made up of the subtraction of the actual load voltage and its reference plus the derivative of this subtraction. Different from the existing SMC methods, in the proposed method the sliding manifold is only the error of the inductor current and its reference without adding the derivative term, which leads to simplification in the calculations and simulation. This control methodology makes use of two cascaded control loops, which are the current control, and the voltage control loops. The voltage control loop generates the inductor current reference and injects it to the sliding mode control block. The sliding manifold and its derivative are defined as follows

$$\sigma = x_1 \tag{12}$$

$$\dot{\sigma} = \dot{x}_1 = f + gu + d(t). \tag{13}$$

To guarantee the stability of the system with the proposed scheme, the subsequent inequality should be discussed to be satisfied:[26]

$$\sigma\dot{\sigma} = \sigma(f + gu + d(t)) \leq -\eta|\sigma| \tag{14}$$

where η is a very large positive coefficient. According to the Lyapunov stability theory, the control input should be designated to guarantee that $\sigma\dot{\sigma}$ is sufficiently negative. If the control input is considered as

$$u = g^{-1}(-f - ksign(\sigma)), \tag{15}$$

substituting (15) in (14) leads to the following equation

$$\sigma\dot{\sigma} = \sigma(-ksign(\sigma) + d(t)) \leq -\eta|\sigma|. \tag{16}$$

If the limit of the disturbances is considered as

$$d(t) \leq D \tag{17}$$

then one can get the limit of *k* for the existence condition as follows

$$k \geq \eta + D. \tag{18}$$

Since η is a very large constant, selecting a large enough value for *k* can stabilize the system. Moreover, the coefficient *k* influences the speed of dynamic response and also the chattering. Even though, choosing a very large *k* value can decrease the response time, but the magnitude of the control input will increase which leads to an increment in chattering. The derived inequality in (18) shows the limit of *k* to stabilize the system with certain parameters. If the system has uncertainty in the parameters of f and g, the estimated values of them as $\hat{f}$ and $\hat{g}$ can be replaced in the mathematical equations. The estimation error of f is supposed to be restricted by an identified function $F = F(x_2)$ where the following equation holds

$$\left|\hat{f} - f\right| \leq F. \tag{19}$$

On the other hand, the control gain (g) is also uncertain with known boundaries as following

$$0 \leq g_{\min} \leq g \leq g_{\max}. \tag{20}$$

Therefore, g is considered as the geometric mean of the boundaries as

$$\hat{g} = \sqrt{g_{\min} g_{\max}}. \tag{21}$$

In other words, one can obtain

$$g\hat{g}^{-1} \leq \sqrt{\frac{g_{\max}}{g_{\min}}} = G. \tag{22}$$

Considering the mentioned uncertainties, $\hat{f}$ and $\hat{g}$ are replaced in (15), then the modified control input is deduced as

$$u = \hat{g}^{-1}(-\hat{f} - ksign(\sigma)) \tag{23}$$

$$\hat{g}^{-1} = \frac{L}{V_{in}} \tag{24}$$

where $\hat{g}^{-1}$ is a positive constant value and the existence is guaranteed. On the other hand, due to the uncertainties in f and g, the existence condition for the boundaries of *k* should be defined again based on the variations. After performing the same calculations as before, the result can be given as

$$k \geq G(F + \eta + D) + (G-1)\left|-\hat{f}\right|. \tag{25}$$

Because F is a function of x_2, therefore the value of k is also a function of x_2 and can be selected as:

$$k(x_2) = G(F + \eta + D) + (G-1)\left|-\hat{f}\right|. \tag{26}$$

Therefore, replacing the modified k in (23), the final control input to the system under the uncertainty can be written as

$$u = \hat{g}^{-1}(-\hat{f} - k(x_2)sign(\sigma)) \tag{27}$$

4. VARIABLE BOUNDARY LAYER

Against the significant features of the SMC method, it suffers of the chattering phenomena. Chattering can stimulate the system on high frequencies and unstable the whole system. Therefore, most of the control methods aim to alleviate the chattering and smooth the control input. The boundary layer method can reject the chattering by limiting the high frequency fluctuations of the sliding manifold in a boundary layer adjacent the switching manifold as follows [26]

$$B(t) = \left\{x \middle| \sigma(x,t) \leq \varphi\right\} \qquad \varphi \geq 0 \tag{28}$$

where φ is the thickness of the boundary layer. To adopt the boundary layer method to the controller, it is adequate to substitute the sign function with the saturation function in (27) as follows

$$u = \hat{g}^{-1}(-\hat{f} - k(x_2)sat(\frac{\sigma}{\varphi})). \tag{29}$$

In order to maintain stability and preserve the existence conditions, (14) should be modified. In other words, the attractiveness of the sliding manifold with boundary layer should be also guaranteed. Thus, the new existence condition is obtained as [26]

$$|\sigma| \geq \varphi \qquad \sigma\dot{\sigma} \leq (\dot{\varphi} - \eta)|\sigma|. \tag{30}$$

According to the new existence condition in (30), *k* should also be modified. Hence, the modified variable limit is found as

$$\bar{k}(x_2) \geq G(F + \eta + D) + (G-1)\left|-\hat{f}\right| - G\dot{\varphi}. \tag{31}$$

Therefore, $\dot{\varphi}$ should be also added to the control gain and the modified *k* as the function of x_2 is attained as

$$\bar{k}(x_2) = k(x_2) - G\dot{\varphi}. \tag{32}$$

Assuming that the sliding manifold is inside the boundary layer, then the following equation holds [26]

$$|\sigma| < \varphi \Rightarrow sat(\frac{\sigma}{\varphi}) = \frac{\sigma}{\varphi}. \tag{33}$$

Therefore, the derivative of the sliding manifold when it is confined to the boundary layer can be obtained as

$$\begin{aligned} \dot{\sigma} &= f(x_2) + G(-\hat{f}(x_2) - \bar{k}(x_2)\frac{\sigma}{\varphi}) + d(t) \\ &= -G\bar{k}(x_2)\frac{\sigma}{\varphi} + \Delta f(x_2) + d(t) \end{aligned} \tag{34}$$

where

$$\Delta f(x_2) = f(x_2) - G\hat{f}(x_2). \tag{35}$$

Replacing (4) in (34) yields

$$\dot{\sigma} = (-G\bar{k}(v_o^*)/\varphi)\sigma + \Delta f(v_o^*) + d(t) + \psi(v_o) \tag{36}$$

where

$$\psi(v_o) = (G\bar{k}(v_o)/\varphi)\sigma - \Delta f(v_o). \tag{37}$$

Now, the Laplace transform of (36) results in

$$\sigma(s) = \frac{\Delta f(v_o^*) + d(s) + \psi(v_o)}{s(s + G\bar{k}(v_o^*)/\varphi)} \tag{38}$$

where s is the Laplace operator. Close inspection to (38) reveals that the variable boundary layer method is removing the high frequency ripples by assigning a low-pass filter to the dynamics of the sliding manifold. The time constant of the first order equation showing the dynamic of the sliding manifold is given by

$$\frac{G\bar{k}(v_o^*)}{\varphi} = \tau. \tag{39}$$

On the other hand, τ is also the bandwidth of the low pass filter which can be selected based on the high frequencies in the system. The final dynamic of the variable boundary layer can be written as

$$\dot{\varphi} + \tau\varphi/G^2 = k(v_o^*)/G \tag{40}$$

where

$$k(v_o^*) = G(F(v_o^*) + \eta + D) + (1-G)\left|\hat{f}\right|. \tag{41}$$

Hence, the final control input under the uncertainties and variable boundary layer is given by

$$u = \hat{g}^{-1}(-\hat{f}(x_2) - \bar{k}(x_2)sat(\frac{\sigma}{\varphi})) . \tag{42}$$

5. REFERENCE GENERATION

The outer control loop is the voltage controller which is tuned based on using the proportional-resonant (PR) controller. In this method, the input to the controller is the second state variable (x_2) and the output of the controller produces the inductor current reference which will be injected to the current control loop. The transfer function of PR controller is given by

$$G_{PR}(s) = K_P + \frac{2K_R\omega_c s}{s^2 + 2\omega_c s + \omega_0{}^2} \tag{43}$$

where K_P and K_R are the proportional and the resonant constants respectively. ω_0 signifies the fundamental angular frequency and ω_c is the cut-off frequency. Tuning the parameters of the PR transfer function achieves the desired phase and gain margin to stabilize the system while generating the desired inductor current reference.

6. SIMULATION RESULTS

In this section, the efficiency of the proposed strategy is investigated in MATLAB/Simulink to certify the theoretical results. The block diagram of the sliding mode control with the proposed variable boundary layer is depicted in Figure 2. As one can see, the output voltage and the inductor current are sensed and transferred to the control block.

First of all, a PR controller is leveraged to regulate the output voltage while generating the inductor current reference. Then the sliding function is generated from the difference of the inductor current and its reference. After that the variable boundary layer is generated through (40) and given to the sliding function to generate the control input. Since the boundary layer is variable, thus the sliding coefficients are also functions of time and implemented to the control input. Finally, the control input is injected to the PWM block to generate the pulses of the H-bridge inverter.

To verify the effectiveness of the proposed method over the existing ones, this scheme is compared to conventional SMC, SMC with constant boundary layer and the STSMC in the upcoming subsections. The only variation in Figure 2 for the other methods is to change the control input equation. In the first subsection, a conventional SMC without applying any chattering alleviation is presented. After that, in the second subsection a sliding mode control with a constant boundary layer is analyzed. The proposed scheme with variable boundary layer is simulated and the results are inspected in the third subsection and in the final subsection the simulation results of the STSMC is obtained and analyzed. Moreover, the amount of the circuit and control parameters are given in Table 1.

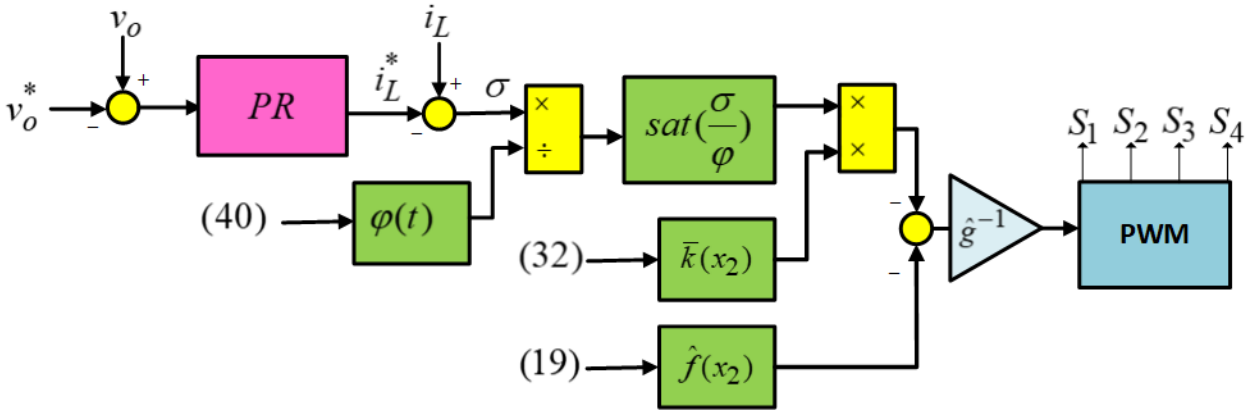

Figure 2. *Block diagram of the control method with variable boundary layer thickness*

Table 1. *System and Control Parameters*

Parameter	Value
Input dc voltage (V_{in})	300 V
Filter inductance (L)	250 μH
Filter capacitance (C)	100 μF
Load ($R + jX$)	$50 + j0.942\Omega$
Output voltage reference (Magnitude) (V_o^*)	200 V
Nominal frequency (f_g)	50Hz
η	2000
D	1000
τ	500
α, β	0.84,0.77
k_p, k_r, ω_c	1, 1500,1

6.1. Performance without Boundary Layer

Considering 20% mismatch in the input voltage (V_{in}) and 40% mismatch in the inductor and capacitor values, the boundaries of unknown parameters can be estimated in advance. The estimated values are calculated as follows

$$\hat{g} = \sqrt{g_{\min} g_{\max}} = 41 \times 10^3$$

$$G = \sqrt{\frac{g_{\max}}{g_{\min}}} = 1.86$$

$$\hat{f}(x_2) = -4000 x_2$$

$$F = 6.7 \times 10^3 |x_2|$$

$$d(t) = \frac{-v_o^*}{L} - i_L^* < \left|\frac{-v_o^*}{L}\right| + \left|i_L^*\right| = D$$

where D can be selected as a large value to satisfy the conditions. According to (27), the control input is $u = 24\times10^{-5}\left[4000x_2 - k(x_2)sign(\sigma)\right]$ where $k(x_2) = 1.86\left(F + \eta + D\right) + 0.86\left|-\hat{f}\right|$.

Figure 3 shows the control input (u), the tracking error (x_1) which is identical to sliding function and the load voltage and current obtained by the control input without boundary layer. All the chattering alleviation methods use a compromise between the chattering magnitude and the steady state error. Therefore, for comparing different methods, the steady state error is kept approximately equal to 0.2 A peak to peak and the control inputs with the defined steady state error are depicted. In Figure 3 (a) the control input is shown, and the large value of chattering originates from the sign function. If the high frequency ripple of the chattering phenomena is calculated as a percentage of the peak-to-peak magnitude of the control input, then this method has 50% high frequency ripple over the control input. Moreover, Figure 3(c) displays the successful simultaneous performance of the cascaded PR controller and SMC to generate a sinusoidal load voltage while tracking the reference with the least error.

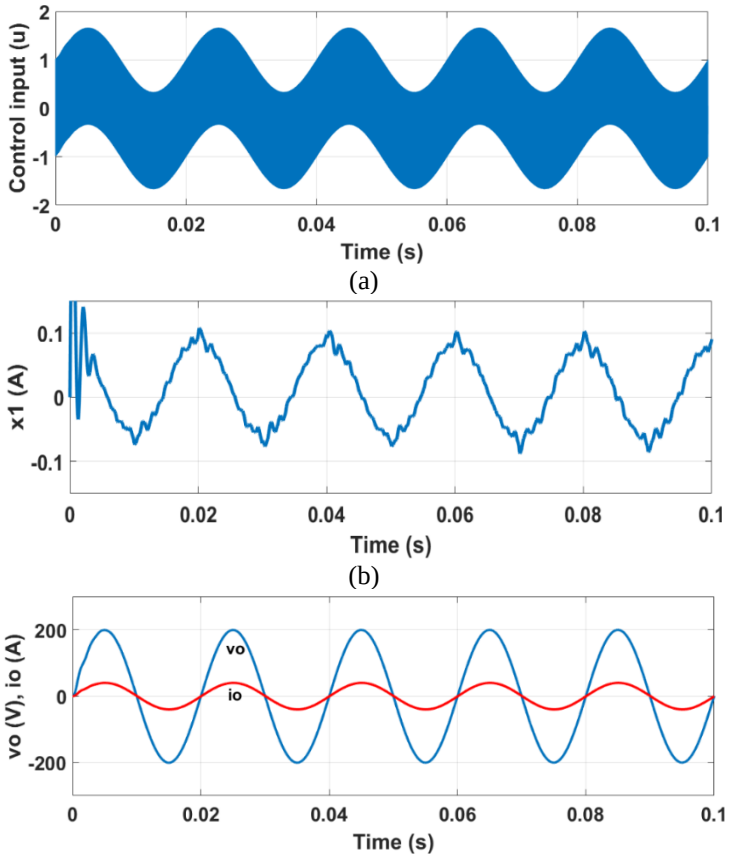

Figure 3. *Control input, steady state error and load voltage and current obtained by SMC without boundary layer (a) Control input (u) (b) Steady state error (x_1) (c) Load voltage and current (v_o, i_o)*

6.2. Performance With Constant Boundary Layer

In the constant boundary layer method, (29) is applied to the circuit as the control input. The amount of the boundary layer thickness is considered as $\varphi = 10$ by trial and error to optimize the least chattering while the peak-to-peak magnitude of the steady state error is 0.2 A and instead of the sign function, the saturation function is used to limit the sliding manifold inside the boundary layer.

Figure 4 depicts the results of the control scheme obtained by the constant boundary layer. Comparing Figure 3 and Figure 4, one can see that the fluctuations of the control input are decreased significantly for the constant boundary layer case in such a way that it has decreased to 8.33% of the peak-to-peak magnitude

of the control input. On the other hand, Figure 4(c) depicts that decreasing the chattering phenomena can influence the output voltage distortion and increases the THD. Hence, in order to decrease the ripples and at the same time keep the steady state error at a very small value and getting a better THD, a variable boundary layer method is applied to circuit in the next sub-section.

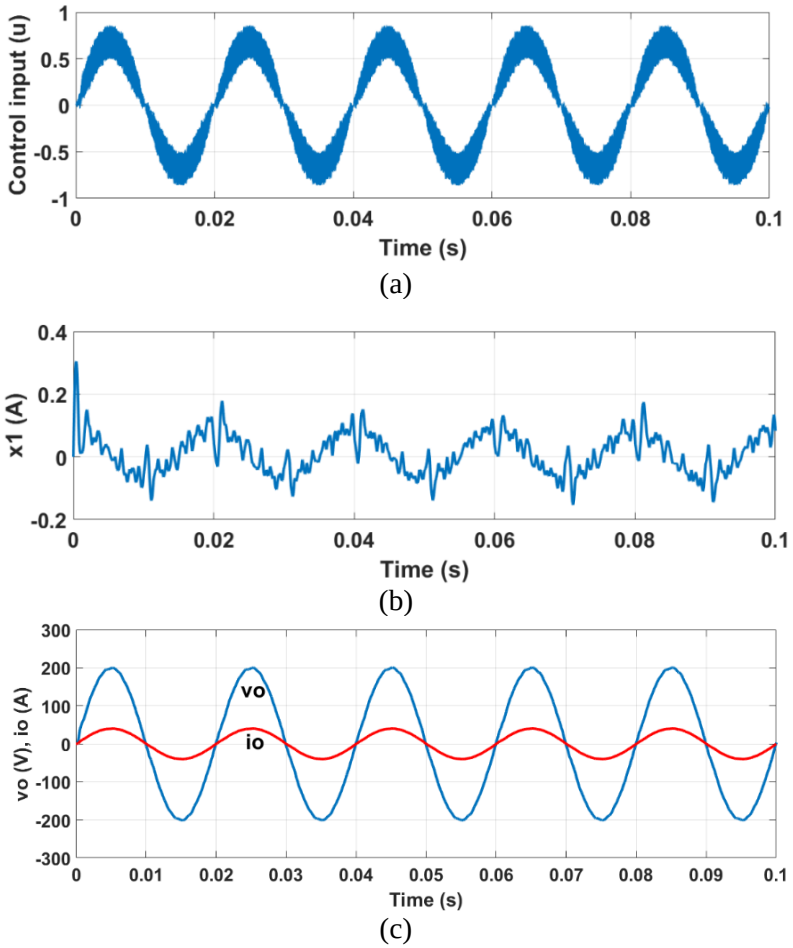

Figure 4. *Control input, steady state error and load voltage and current obtained by SMC with constant boundary layer: (a) Control input (u) (b) Steady state error (x_1) (c) Load voltage and current (v_o, i_o)*

6.3. Performance With Variable Boundary Layer

In the variable boundary layer method (42) is applied to the system as the control input. The amount of $k(v_o^*)$ is calculated as follows

$$k(v_o^*) = 1.86\left(F + \eta + D\right) + 0.86\left|-\hat{f}\right|$$
$$= 1.86\left(6.7\times10^3\left|v_o^*\right| + \eta + D\right) + 0.86\left|-\hat{f}\right|$$

where $v_o^* = 200\sin(\omega t)$ and $\omega = 2\pi f_g$. The control input, steady state error and load voltage and current with variable boundary layer are depicted in Figure 5. Comparing Figure 5 with Figure 4 and Figure 3, one can observe that the chattering is eliminated completely with the variable boundary layer so that the ripples over the control input is reduced to 3.33% of the control input magnitude. On the other hand, the error is suppressed significantly while the distortion of the load voltage is also improved.

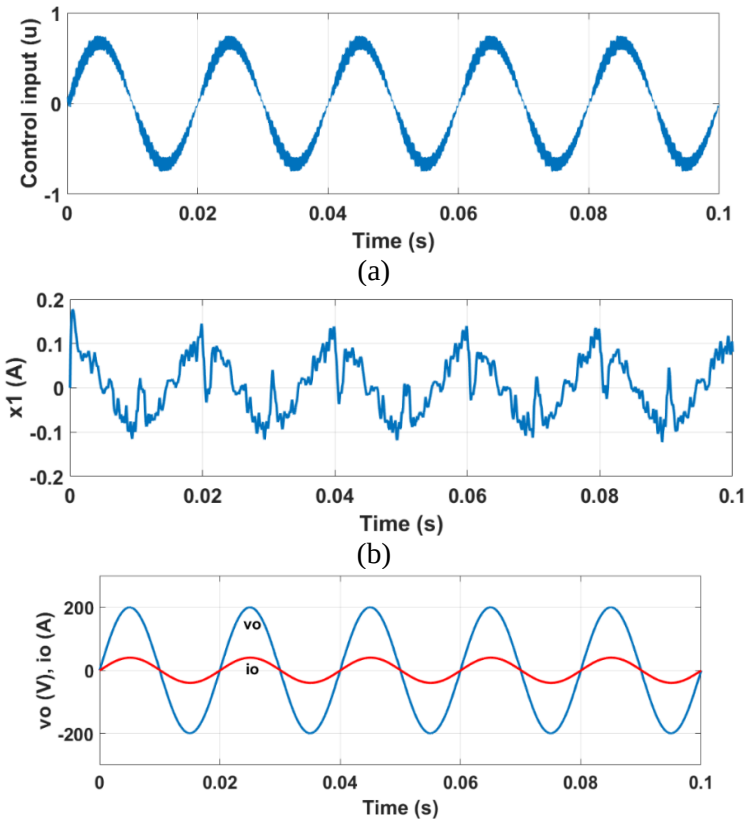

Figure 5. *Control input, steady state error and load voltage and current obtained by SMC with variable boundary layer: (a) Control input (u) (b) Steady state error (x_1) (c) Load voltage and current (v_o,i_o)*

The robustness of the suggested control scheme under parameter mismatch in the input voltage and the inductor (*L*) and capacitor (C) is investigated in Figure 6. In Figure 6(a), the voltage source inverter operates at input voltage perturbation between 240-300 V, while the other parameters are kept same, and the load voltage and current are depicted in steady state. In Figure 6(b), simulated load voltage and current are given when there is -40% mismatch in the *L* and C parameters. Obviously, the output voltage is not affected from these disturbances in both cases.

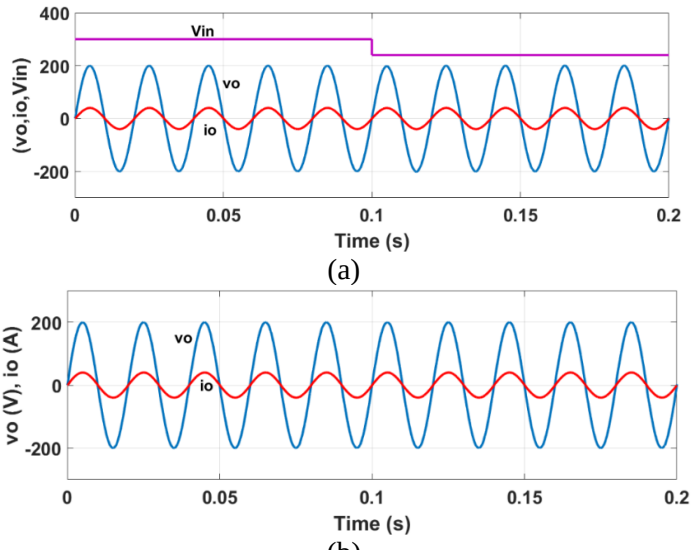

Figure 6. *Output voltage and current obtained by: (a) when $\hat{V}_{in}$ is different from V_{in} by -20%, (b) when $\hat{L}$ and $\hat{C}$ are different from L and C by -40%*

The performance of the method under nonlinear load is shown in Figure 7. It is shown that the controller persists generating a sinusoidal output voltage with the least THD. The THD of the load voltage obtained by the constant and variable boundary layer methods are 1.95% and 1.53%, respectively. Clearly, the variable boundary layer performs better in keeping the THD in a small value under a nonlinear load. However, both THD values are below the IEEE standard limits.

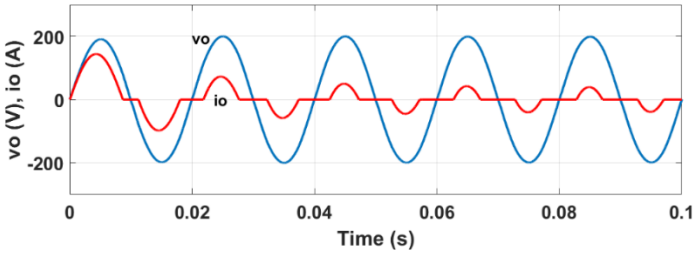

Figure 7. *load voltage and current under nonlinear load.*

The switching frequency and the output voltage and current under load variation are depicted in Figure 8. Figure 8(a) demonstrates that the proposed method achieves fixed switching frequency by limiting the chattering inside a boundary layer thickness even while a dynamic change exists in the system, and Figure 8(b) depicts the load voltage and current and the variation in load current.

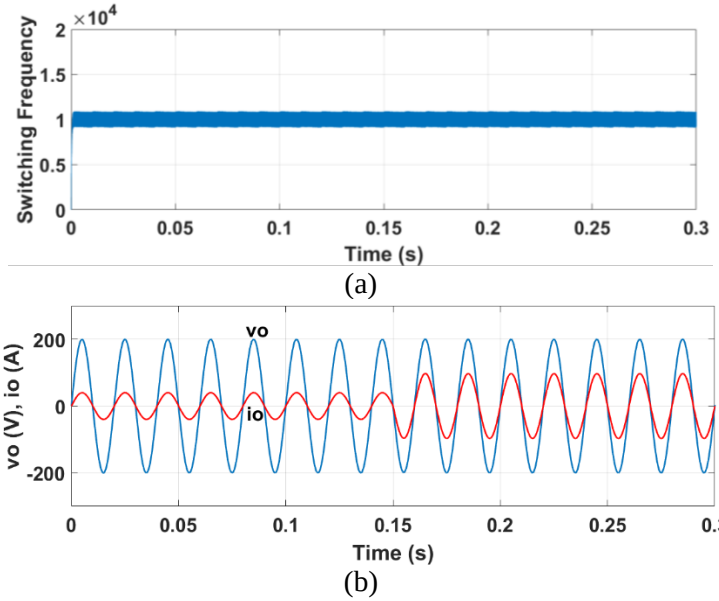

Figure 8*. Switching frequency during load variation at t=0.15 s (a) switching frequency (b) load current.*

6.4. Performance With STSMC

Since the STSMC method has received great attention in chattering alleviation, this strategy is selected for comparing with the proposed strategy in this paper. The control law of the STSMC is given as follows [25]

$$u_{ST} = -\alpha\sqrt{|S|}sign(S) + v_{ST}$$
$$\dot{v}_{ST} = -\beta sign(s) \tag{44}$$

where α and β are the constant coefficients. For applying this control input to the single-phase voltage source inverter, (44) is substituted in (23) to satisfy the Lyapunov condition. The resultant control input that should be applied to the system is as follows

$$u = \hat{g}^{-1}(-\hat{f} - u_{ST}) \quad (45)$$

The control input and the steady state error under the STSMC are depicted in Figure 9. Comparing Figure 9 (a) with Figures 3 ,4 and 5 shows that the control input of the variable boundary layer method in the same magnitude of the steady state error has less chattering while the chattering over the control input of the STSMC is 10% of the control input magnitude. Therefore, the proposed method is more efficient to remove the chattering however according to Figure 10, the THD measured for STSMC is less than the other methods.

For comparing the methods in terms of the number of coefficients that should be tuned, the constant boundary layer method needs to tune the boundary layer thickness, however the variable boundary layer thickness is adaptive to the system variations and doesn't need to be tuned manually. On the other hand, the STSMC has two coefficients that need to be regulated according to the system conditions.

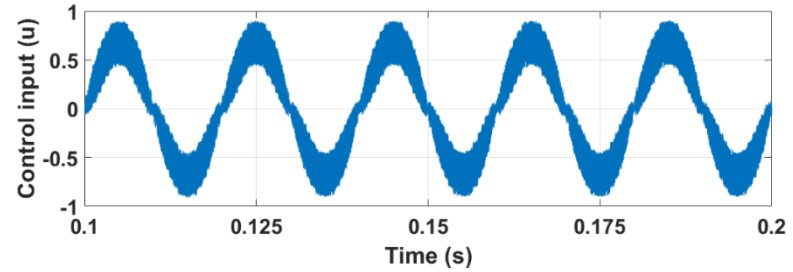

(a)

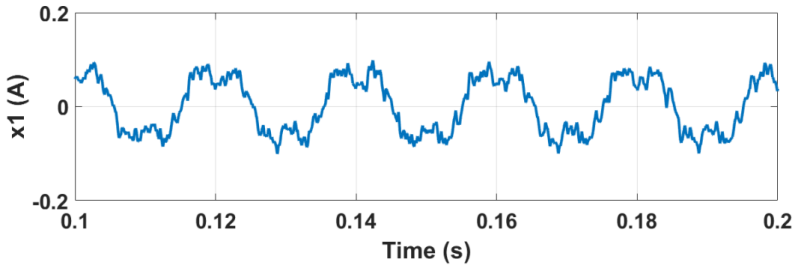

(b)

Figure 9. *Control input and steady state error obtained by STSMC: (a)control input (u) (b) inductor current error (x_1)*

Moreover, the THDs of output voltages obtained with these methods under a nonlinear load are given in Figure 10. According to Figure 10(a), the constant boundary layer method has the largest THD value while the proposed method and STSMC methods show approximately better THD values than the constant boundary layer method.

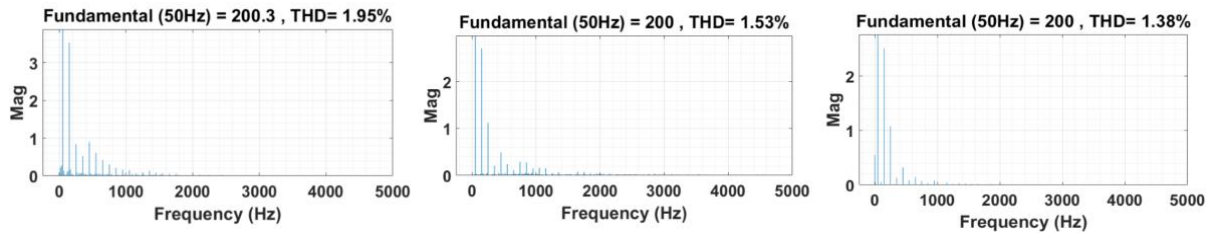

(a) (b) (c)

Figure 10. *Total harmonic distortion under a nonlinear load: (a) constant boundary layer method, (b) variable boundary layer method (c) STSMC method*

7. CONCLUSION

In this paper, an adaptive sliding mode control with variable boundary layer methodology is proposed for single-phase voltage source inverters. For controlling the load voltage of the standalone single-phase inverter, two control loops are introduced. The voltage control loop generates the inductor current reference and injects it to the current control loop. The latter loop is operating based on a variable boundary layer SMC and generates the control input to the pulse width modulation (PWM) block.

On the contrary to the conventional fixed boundary layer methods, the variable boundary layer doesn't need to be tuned manually and can be varied adopted to the system variations to bound the chattering inside a boundary layer. The proposed variable boundary layer not only eliminates chattering, but also attains to the minimum steady state error in the load voltage while also it has a self-regulation characteristic. The efficiency of the control strategy is compared with the other methodologies which do not use boundary layer, use constant boundary layer and STSMC method. Simulation results demonstrate that the variable boundary layer scheme decrements the chattering from 50% in the conventional SMC ,8% in constant boundary layer and 10% in STSMC method to 3% while keeping the same steady state error for all the methods.

CONFLICTS OF INTEREST

No conflict of interest was declared by the authors.

REFERENCES

[1] Abdel-Rahim, N. M., Quaicoe, J. E., "Analysis and design of a multiple feedback loop control strategy for single-phase voltage-source UPS inverters", Power Electron IEEE Transaction, 11(4): 532–541, (1996).

[2] Hao, M., Longyu, C., Zhihong, B., "An active-clamping current-fed push-pull converter for vehicle inverter application and resonance analysis", IEEE Internatioal Symposium, Industrial Electron, Hangzhou, China , (2012).

[3] Deng, H., Oruganti, R., Srinivasan, D., "A simple control method for high-performance UPS inverters through output-impedance reduction", In IEEE Transactions on Industrial Electronics, 55(2): 888–898, (2008).

[4] Chenlei, B., Xinhua, R., Xuehua, W., "Design of grid-connected inverters with LCL filter based on PI regulator and capacitor current feedback active damping", 2012 IEEE Energy Conversion Congress and Exposition (ECCE), Raleigh, (2012).

[5] Komurcugil, H., Altin, N., Ozdemir, S., Sefa, I., "Lyapunov-function and proportional-resonant-based control strategy for single-phase grid connected VSI with LCL filter", IEEE Transactions on Industrial Electronics, 63(5): 2838–2849, (2016).

[6] Tzou, Y.Y., Ou, R.S., Jung, S.L., Chang, M.Y., "High-performance programmable ac power source with low-harmonic distortion using DSP based repetitive control technique", In IEEE Transactions on Power Electronics, 12(4): 715-725, (1997).

[7] Zhang, K., Kang, Y., Xiong, J., Chen, J., "Direct repetitive control of SPWM inverter for UPS purpose", In IEEE Transaction on Power Electronics, 18(3): 784-792, (2003).

[8] Rech, C., Grundling, H., Pinheiro, J. R., "A modified discrete control law for UPS applications", IEEE 31st Annual Power Electronics Specialists Conference, Conference Proceedings, Galway, Ireland, 3: 1476-1481, (2000).

[9] Zhang, X., Wang, Y., Yu, C., Guo, L., Cao, R., "Hysteresis model predictive control for high-power grid-connected inverters with output LCL filter", In IEEE Transactions on Industrial Electronics, 63(1): 246–256, (2016).

[10] Baghaee, H.R., Mirsalim, M., Gharehpetian, G.B., Talebi, H.A., "A decentralized robust mixed H2/H ∞ voltage control scheme to improve small/large-signal stability and FRT capability of islanded multi-DER microgrid considering load disturbances", In IEEE Systems Journal, 12(3): 2610-2621, (2018).

[11] Kawamura, A., Chuarayaratip, R., Haneyoshi, T., "Deadbeat control of PWM inverter with modified pulse patterns for uninterruptible power supply", IEEE Transaction Industrial Electron, 35(2): 295-300, (1988).

[12] Hua, C., "Two-level switching pattern deadbeat DSP controlled PWM inverter", IEEE Transaction Power Electron, 10(3): 310-317, (1995).

[13] Kukrer, O., Komurcugil, H., "Deadbeat control method for single-phase UPS inverters with compensation of computation delay", In IEE Proceedings, Electric Power Applications, 146(1): 123-128, (1999).

[14] Pascual, M., Garcera, G., Figueres, E., Gonzalez-Espin, F., "Robust Model-Following Control of Parallel UPS Single-Phase Inverters", Industrial Electronics IEEE Transactions, 55(8): 2870-2883, (2008).

[15] Dahono, P.A., Taryana, E., "A new control method for single-phase PWM inverters to realize zero steady-state error and fast response", In Proceeding of 15th International Conference of Power Electron, Drive System, Singapore, (2003).

[16] Woo, Y., Kim, Y.C., "A digital control of a single-phase UPS inverter for robust ac-voltage tracking", In Proceeding 30th Annual Conference of IEEE Industrial Electronics Society, IECON 2004, Busan, South Korea, (2004).

[17] Utkin, V., Guldner, J., Shi, J., Sliding mode control in electro -mechanical systems, CRC press, Taylor and Francis Group, (2009).

[18] Abrishamifar, A., Ahmad, A. A., Mohamadian, M., "Fixed Switching Frequency Sliding Mode Control for Single-Phase Unipolar Inverters", IEEE Transaction, Power Electron, 27(5): 2507–2514, (2012).

[19] Makrini, IE., Rodriguez, C., Lefeber, D., Vanderborght, B., "The Variable Boundary Layer Sliding Mode Control: A Safe and Performant Control for Compliant Joint Manipulators", IEEE Robotics and Automation Letters, 2(1): 187-192, (2017).

[20] Levant, A., "Sliding order and sliding accuracy in sliding mode control", International Journal of Control, 58: 6, 1247-1263, (1993).

[21] Guo, B., Su, M., Sun, Y., Wang, H., Dan, H., Tang, Z., Cheng, B., "A Robust Second-Order Sliding Mode Control for Single-Phase Photovoltaic Grid-Connected Voltage Source Inverter", IEEE Access,7: 53202-53212, (2019).

[22] Lu, J., Savaghebi, M., Ghias, A M.Y.M., Hou, X., Guerrero, J., "A Reduced-Order Generalized Proportional Integral Observer-based Resonant Super twisting Sliding Mode Control for Grid-

Connected Power Converters" In IEEE Transactions on Industrial Electronics, 68(7): 5897-5908, (2021).

[23] Zhang, W., Wang, W., Liu, H., Xu, D.," A Disturbance Rejection Control Strategy for Droop-Controlled Inverter Based on Super-Twisting Algorithm" IEEE Access, (7): 27037-27046, (2019).

[24] Luo, W., Zhao, T., Li, X., Wang, Z., Wu, L., "Adaptive super-twisting sliding mode control of three-phase power rectifiers in active front end applications" IET Control Theory & Applications, 13(10): 1483-1490, (2019).

[25] Utkin, V., "Discussion Aspects of High-Order Sliding Mode Control", IEEE Transactions on Automatic Control, 61(3): 829-833, (2016).

[26] Slotine, J., Li, W., Applied Nonlinear Control Prentice-Hall Englewood Cliffs, New Jersey, (1991).